Drying Model for Calcium Alginate Beads[†]

Margaret E. Lyn*[,‡] and DanYang Ying[§]

US Department of Agriculture, Agricultural Research Service, Application & Production Technology and Biological Control of Pests Research Units, Stoneville, Mississippi 38776, and CSIRO Food and Nutritional Science, 671 Sneydes Road, Werribee, Melbourne, VIC3030, Australia

The dehydration of calcium alginate beads is observed to have a simple power-law time dependence. The ratio of the water content, $M(t)$, to the initial water content, M_0, can be expressed as

$$M(t)/M_0 = (1 - t/t_c)^{32}$$

The parameter t_c is insensitive to the guluronic content of the alginate or the degree of cross-linking. Using this simple model, t_c can be estimated from the properties of water vapor, the initial water content, and the relative humidity, in addition to an empirically derived correction factor, K, which has been found to be 2.8 ± 0.3.

Introduction

Obtained from certain types of brown seaweed, the natural polymer called alginate has widespread applications in the food,[1−3] pharmaceutical,[4,5] cosmetics, medical,[6] and biotechnology[7,8] industries. One of the outstanding features alginate offers is the instant gelling property when the alginate solution is in contact with Ca^{2+} or other di- and trivalent cations, which induce instant cross-linking.[5,9−11] This feature is why alginate is frequently used for cell immobilization and microencapsulation of a wide range of bioactives.

Our particular interest is the use of this material to encapsulate bioactives and especially, living beneficial microbiological agents for the control of agricultural pests.[12] An important step in such a formulation is the drying of calcium alginate beads containing the bioactives to a low water content appropriate for long-term storage. A simple model that describes most of the drying process could be useful in this and other applications requiring dried alginate beads. Research areas involving the development of agricultural biocontrol formulations, drug delivery systems,[13] and probiotic foods[14−18] where alginate beads containing immobilized cells and other bioactive compounds are air-dried would benefit from a drying model that could describe the drying process to nearly 100% water mass loss.

Availability of a model to estimate either the time duration necessary to reach an optimal moisture content or the conditions to achieve a desired drying time would be beneficial. Such a model could contribute to the development of an efficient evaluation phase in the research and development of air-dried alginate products or to the optimization of processing times in industrial applications. However, a review of the literature on the drying of gels[19−24] suggests that no simple model can be used to describe the entire drying process. In this paper, we point out that for the specific case of calcium alginate beads, nearly the entire process can be described with the simple model described herein.

Model of Bead Dehydration

It will be assumed that the loss of mass of a drying bead is governed by the diffusion of saturated water vapor at the surface of the bead into the surrounding air at ambient relative humidity. As such, the water loss is given by the Fickian laws of diffusion assuming spherical symmetry. If C_{sat} is the concentration of water vapor at the surface of a bead with radius R and C_{amb} is the water vapor concentration at a distance l from the center of the sphere, then the steady solution to the diffusion equation gives the concentration of water vapor, $C(r)$, at an arbitrary distance, r, as[25]

$$\frac{C_{sat} - C(r)}{C_{sat} - C_{amb}} = \frac{(r - l)R}{(R - l)r}$$

The quantity of water vapor leaving the surface per unit time is[26]

$$dM/dt = -4\pi D_v(C_{sat} - C_{amb})Rl/(l - R)$$

where D_v is the diffusion coefficient of water vapor in air. For $l \gg R$, the condition to be used for experiments,

$$dM/dt = -4\pi D_v(C_{sat} - C_{amb})R$$

or in terms of relative humidity, R_h,

$$dM/dt = -4\pi D_v C_{sat}(1 - R_h/100)R \quad (1)$$

The mass of a bead or droplet of water in terms of its density and an additional factor, f, is

$$M = 4/3\pi R^3 \rho f \quad (2)$$

where ρ is the density of beads, which is very close to that of water, 1.0 g·cm^{-3}. The origin of the factor f, a truncation factor, is described below.

For comparison with theory, the bead in an experiment should maintain a well-defined shape during drying. Ideally, that shape should be spherical; however, a spherical shape cannot be obtained if the bead is to be supported on a flat surface. Under such circumstances, the shape can be approximated as a

[†] Mention of trade names or commercial products in this article is solely for the purpose of providing specific information and does not imply recommendation or endorsement by the U.S. Department of Agriculture.

* To whom correspondence should be addressed. E-mail: margaret.lyn@ars.usda.gov. Phone number: (662) 686-3641. Fax number: (662) 686-5281.

[‡] US Department of Agriculture.

[§] CSIRO Food and Nutritional Science.

10.1021/ie901451m
Published on Web 01/21/2010

truncated sphere with the degree of truncation being determined by the hydrophobicity of the support surface. A suitable surface for use in experiment is Teflon for which the contact angle is large.

According to Lee et al., the volume of a sphere truncated at a surface with contact angle θ is[27]

$$V = 4/3\pi R^3 B^2(3 - 2B)$$

where

$$B = 1/2(1 - \cos\theta)$$

For a bead or water droplet with a contact angle of 110° on a Teflon surface,

$$V = 4/3\pi R^3 \times 0.75$$

That is, for a bead or water droplet supported on a Teflon surface, the appropriate value of the truncation factor, f, is 0.75.

Solving eq 2 for R and substituting into eq 1 gives

$$dM/dt = -4\pi D_v C_{sat}(1 - R_h/100)(4/3\pi\rho f)^{-1/3} M^{1/3}$$

which, on integration, gives

$$\frac{M}{M_0} = \left(1 - \frac{t}{t_c}\right)^{3/2} \quad (3)$$

where M_0 corresponds to an initial water mass when $t = 0$ and

$$t_c = \frac{3\left(\frac{4}{3}\pi\rho M_0^2 f\right)^{1/3}}{8\pi D_v C_{sat}(1 - R_h/100)} \quad (4)$$

Here an additional factor, K, will be included to emphasize the influence of several effects not explicitly included in our simple model. Therefore, eq 4 may be rewritten as

$$t_c = K\frac{3\left(\frac{4}{3}\pi\rho M_0^2 f\right)^{1/3}}{8\pi D_v C_{sat}(1 - R_h/100)} \quad (5)$$

The value of K, which can be viewed as an empirical scaling factor, is assumed to be constant for all values of relative humidity. This empirical scaling factor K accounts for the fact that the bead is on a surface which will result in nonspherical water vapor isobars. In addition, K accounts for a bead temperature that is lower than ambient temperature due to evaporative cooling.

For water at a temperature of 25 °C and normal atmospheric pressure, $D_v = 0.256$ cm^2·s^{-1} and $C_{sat} = 23$ g·m^{-3}.[28,29] Using these values in eq 5 and $K = 2.8$, Figure 1 shows how t_c can be expected to depend on M_0 and R_h. Such a plot may be used to predict experimental t_c values using measurable experimental parameters. For example, beads with an initial water mass of 15 mg in air at 50% relative humidity is expected to reach mass equilibrium within $150 < t_c < 200$ min or in approximately 175 min.

In this paper, the dehydration kinetics of calcium alginate beads will be experimentally investigated and the above drying model will be applied to beads air-dried under different experimental conditions of M_0 and R_h. Further, the validity of the model for applications of alginate with different guluronate content will be investigated and the effect of bead size will also be discussed.

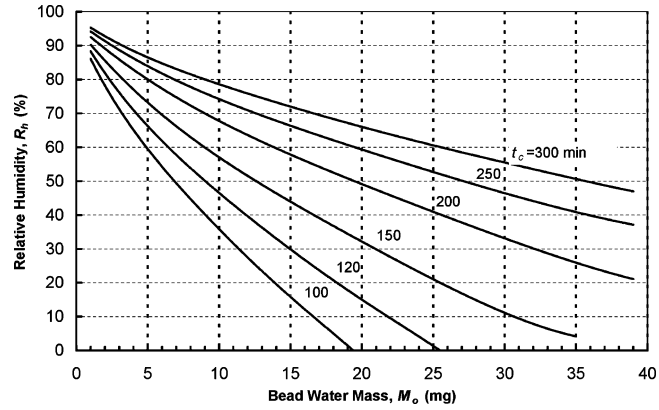

Figure 1. Calculated dependence of t_c on relative humidity and initial water mass.

Materials and Methods

Preparation of Calcium Alginate Beads. A 1% (w/v) sodium alginate solution was added dropwise to a dilute calcium chloride solution from a 10 mL syringe fitted with a 16 gauge needle 3.8 cm in length. Sodium alginate droplets freefell a distance of ~3.8 cm, measured from the needle tip to liquid surface, into the unstirred dilute calcium chloride solution or so-called curing bath. Specific details are described.

The 1% (w/v) sodium alginate solution was prepared as follows: Approximately 5.0 g of Kelgin HV (ISP Alginates), sodium alginate with a 39% guluronic content, was dissolved in 500 mL of deionized water. The mixture was stirred overnight with a stir bar to allow dissolution of the alginate salt.

A saturated calcium chloride $CaCl_2$ solution at 24 °C was prepared by adding an excess of 75 g of $CaCl_2$ to 100 mL of deionized water. Two 10.00 mL aliquots of the saturated $CaCl_2$ solution were quantitatively transferred to a 1.0 L volumetric flask and brought to volume with deionized water. The curing bath was prepared by transferring 100 mL of the dilute $CaCl_2$ solution to a 175 mL, 7.6 cm diameter crystallization dish. In less than 2 min, approximately 1.7−2.0 mL 1% (w/v) sodium alginate was added to the curing bath in droplets totaling 60−70 beads. Collision between incoming droplets and existing beads was avoided by laterally moving the needle above the surface of the dilute $CaCl_2$ solution.

The curing time, or cross-linking time, of 1% (w/v) sodium alginate droplets in calcium chloride was monitored with a stop watch. Sodium alginate droplets, now calcium-cross-linked alginate beads, remained in the curing bath for 80 min without stirring. After ~6 min in the curing bath, the bead density became greater than the $CaCl_2$ solution and the beads sank.

After 80 min in the curing bath, the beads were poured into a 56 mm diameter Buchner funnel and rinsed with 250 mL deionized water. The beads were then transferred to a weighing boat where excess water was removed by blotting with kimwipes. Ten beads, qualitatively similar in size, were selected for the dehydration measurements.

Samples A−E were all prepared using the above procedure. To test the effect of curing time on the drying behavior, sample F was prepared using the same procedure but cured for 24 h instead of 80 min as used for curing sample A−F. Sample G was prepared similarly as F but was allowed to swell in deionized water where the mass of each bead nearly doubled. Sample H was prepared using Manugel GHB, with 63%

Table 1. Summary of Sample Properties and Curing Times

sample ID	guluronic content	curing time	diameter
A−E	39%	80 min	*d*
F	39%	24 h	*d*
G	39%	24 h	2*d*
H	63%	80 min	*d*

guluronic content, following the same procedure for samples A−E. A summary of sample properties and curing times is shown in Table 1.

Dehydration Kinetics. Different relative humidities, R_h's, were created inside a Mettler Toledo AG 204 analytical balance using ambient conditions or by sealing the draft doors with paraffin and using different saturated salt solutions or phosphorus pentoxide, P_2O_5. P_2O_5 was used to create a 21% and 31% R_h environment. Potassium chloride and potassium sulfate were used to create an R_h of 61% and 75%, respectively. An imperfectly sealed balance prevented the saturated salt solutions equilibrium R_h's from being obtained. The sealed balance was allowed to come to a steady state R_h overnight. A VWR digital hygrometer/thermometer housed inside the balance was used to measure the air temperature and steady state R_h.

Ten beads, similar in size, were selected and transferred to a clean Teflon surface with a known average weight. After isolating the ten beads by a distance of ∼1.7 cm from each other, the beads were quickly transferred to the balance. Mass loss with respect to time was recorded using a Mettler Toledo LC-P45 printer at various time intervals until $\Delta M/\Delta t = 0$.

Results and Discussion

The alginate backbone is characterized by varying block lengths of D-mannuronic (M), L-guluronic (G), and MG acid units whereas the M/G ratio and arrangement of the blocks varies with seaweed type. Dissolution of the sodium salt of alginic acid in water produces polyanionic alginate, which cross-links with various di- and trivalent cations such as Ca^{2+} to produce calcium alginate hydrogels or herein referred to as beads. According to the egg−box model proposed by Rees,[9−11] gel formation occurs via complexation of the cation with consecutive guluronate residues. Therefore to evaluate the validity of the model and applicability to beads with either different guluronic content or M_0, sodium alginate of two different guluronic contents (39% and 63%) were evaluated in addition to beads with different M_0. In all, eight different samples labeled A−H were analyzed (Table 1).

Applicability of the model to the drying of beads with similar guluronate composition and M_0 (samples A−C and E) in air at different relative humidites was first evaluated. The loss of water mass from alginate beads A−C and E as a function of time at four different drying humidities is shown in Figure 2. Experimental data points have been fitted with the 3/2 power law given in eq 3 using the indicated value of t_c. The best fit of these experimental data limited t_c to three significant figures. For each set of beads, the model shows a good fit to the data over most of the drying period. This result indicates that the model appears adequate in describing the drying curve for beads of similar size and guluronic composition under different drying humidities.

The experimental t_c values indicated in Figure 2 were obtained by fitting the curves for up to 99% water mass loss. From here on, this fitting parameter will be denoted as t_c(exp) to distinguish it from the theoretical value, t_c(calc), obtainable from eq 4. The ratio t_c(exp)/t_c(calc), limited to two significant figures by either M_0 or R_h through eq 4, is given as K. This empirical scaling factor, K, was included into the model, as shown in eq 5, to

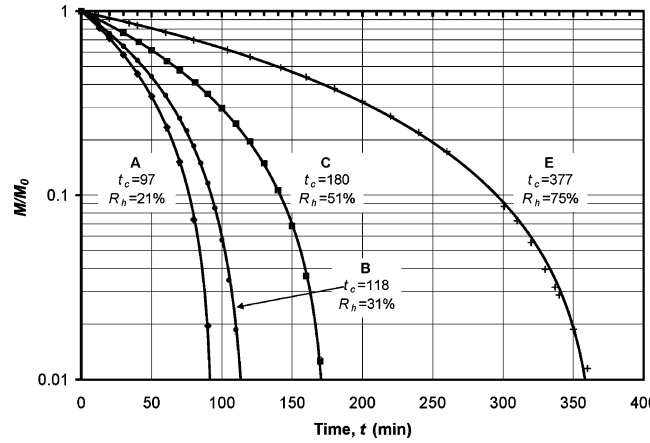

Figure 2. Drying curves for calcium alginate beads with similar guluronate composition and M_0 in air (samples A−C and E) at different relative humidities. The solid lines are a 3/2-power-law fit using the indicated values of t_c.

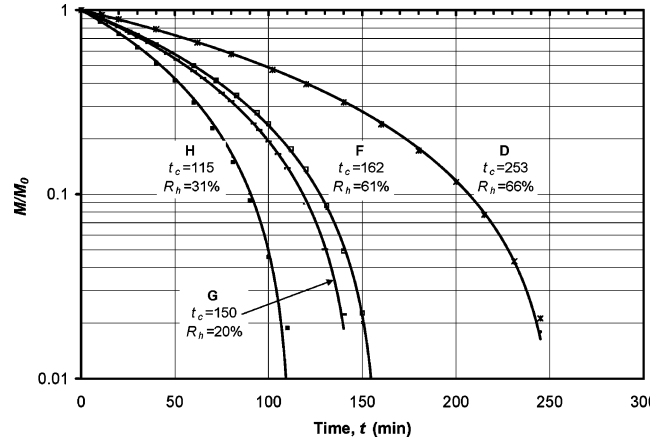

Figure 3. Drying curves for calcium alginate beads with either different guluronic content or different M_0 in air (samples D and F−H) at different relative humidities. The solid lines are a 3/2-power-law fit using the indicated values of t_c.

emphasize the influence of several effects not explicitly included in the simple model and is necessary to bring t_c(calc) into agreement with experimental data.

Since a spherical bead or water droplet on a supporting surface adopts a truncated spherical geometry, nonspherical water vapor isobars and higher water vapor pressures in the restricted space near the droplet−surface interface are to be expected in experiments. In these experiments, the presence of a supporting surface reduces evaporation rates and leads to larger experimental t_c values in comparison to calculated t_c values in which the presence of a surface was not entirely taken into account (eq 4). Unfortunately, inclusion of either a dynamic temperature to account for evaporative cooling or a supporting surface into the model prohibits a simple solution to the diffusion equations. However, semiempirical values of t_c may be predicted using eq 5 with an assumed value of $K = 2.8 \pm 0.3$ (discussed below).

Applicability of the model to beads with either different guluronic content or different M_0 but similar guluronate composition was also evaluated. Figure 3 shows the experimental drying curves for samples D and F−H fitted with the 3/2 power law given in eq 3 using the indicated value of t_c. For these samples, the model shows a good fit to the data over most of the drying period. This observation indicates that the model may also be adequate in describing the drying behavior of beads

Table 2. Best Fit of t_c to Various Dehydration Curves for Beads of Similar Size and Guluronic Content (Samples A−E), Beads of the Same Guluronic Content and Different Sizes (Samples F and G), and Beads with Different Guluronic Content (sample H) Air Dried at the Indicated Relative Humidities at 25 ± 1 °C[a]

		initial				
sample	alginate (%G)	mass, M (mg)	% moisture	R_h (%)	t_c(exp) (min)	K
A	Kelgin HV (39)	14.4	97	21 ± 4	97	2.7
B	Kelgin HV (39)	15.6	97	31 ± 4	118	2.6
C	Kelgin HV (39)	15.1	97	51 ± 2	180	2.9
D	Kelgin HV (39)	13.2	94	66 ± 2	253	3.1
E	Kelgin HV (39)	14.6	97	75 ± 4	377	3.1
F	Kelgin HV (39)	10.5	96	61 ± 2	162	2.6
G	Kelgin HV (39)	29.7	99	20 ± 4	150	2.5
H	Manugel GHB (63)	15.0	97	31 ± 4	115	2.6

[a] The empirical scaling factor, K, is derived from the ratio t_c(exp)/t_c(calc).

with different guluronic composition or initial water mass when air-dried at a mid to low relative humidity.

A summary of t_c(exp) and the empirical scaling factor, K, for the eight different bead samples A−H is presented in Table 2. Dehydration kinetics measurements for each sample were taken at the indicated steady state R_h's. Samples A−C and E are similar in both guluronate composition (39%) and M_0 (∼15 mg) whereas samples D, F, and G are also similar in guluronate content (39%) but differ in initial water mass ranging from 11 to 30 mg. In contrast to samples A−G, sample H was prepared from an alginate with 63% guluronic content.

Despite differences among the samples, no particular trend in either guluronic content or M_0 or R_h could be observed for K (Table 2). In other words, there does not appear to be any relation between the empirical scaling factor K and sample differences arising from alginate type and initial bead size. Consequently, the spread in K as shown in Table 2 may be attributed to indeterminate errors in sample measurements whereas the magnitude of K can be attributed to the presence of a supporting surface in the experiments and by the process of evaporative cooling. As previously discussed, inclusion of either a dynamic temperature to account for evaporative cooling or a supporting surface into the model prohibits a simple solution to the diffusion equations.

The distribution of K values in Table 2 may be averaged to give a value of $K = 2.8 \pm 0.3$ (99% confidence interval) for use in predicting t_c for any arbitrary set of M_0 and R_h using eq 5. Figure 4 presents this confidence interval range for t_c(calc) values for any arbitrary M_0 and R_h. Superimposed on the predicted t_c plot are t_c(exp) values from Table 2, which are represented by open circles. Overall, the semiempirical model appears to predict t_c reasonably well for each of the eight different samples. However, use of the model appears to be more appropriate when drying under mid to low humidity conditions rather than at higher humidities. At mid to high R_h, the model appears to underestimate t_c. This observation can be explained by the relation between t_c and R_h. It can be seen from eq 4 that t_c is a strictly increasing function that is asymptotic to $R_h = 1$. That is, as R_h approaches 100%, t_c approaches infinity. Thus at high relative humidities, small differences between true R_h and measured R_h will lead to larger differences between fitted t_c (based on true R_h) and predicted t_c (based on measured R_h) values in comparison to drying at lower humidities.

While the simple model described herein has been shown to be applicable to calcium alginate beads, the most significant result from this investigation is that all the drying curves for the different calcium alginate beads studied follow the same

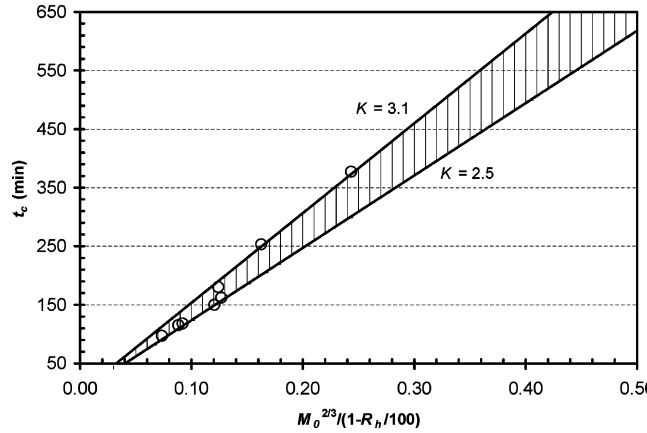

Figure 4. Predicted t_c values for any arbitrary set of M_0 and R_h within the 99% confidence interval limits (shaded zone) for $K = 2.8 \pm 0.3$. Open circles represent experimental data points.

power law, which was derived using a model that should be most appropriate for a pure water droplet since the properties of alginate do not enter into the equations. In fact, an attempt to investigate the drying of a water droplet revealed the following problem. As a truncated spherical water droplet evaporates, it has a tendency to remain pinned to a fixed contact surface. If the contact surface were to remain unchanged while the droplet evaporates, the shape of the droplet would tend toward that of a pancake. Although pinning is only a metastable condition caused by surface irregularities, it did make it difficult to obtain reproducible data for water droplets. For the calcium alginate beads, pinning did not prove to be a problem. The surprising result is that the model developed for a water droplet works better for beads than for water droplets.

More complex models have been necessary for other hydrogels.[30−32] An explanation to account for our observation may be that strong interchain interactions prevent collapse of the barrier layer in the case of alginate hydrogels. It is unclear at this point whether this simple model could be extended to nonalginate hydrogels. This is the first study in a series to develop a simple model to describe the drying of alginate beads for different applications. Additional studies are underway to investigate applicability of the model to alginate beads loaded with starch solids.

Conclusions

It has been shown that the time dependence of water loss from calcium alginate beads, over almost the entire drying range, can be described by a single simple expression, $(1 - t/t_c)^{3/2}$. At 25 ± 1 °C, the model has been found to be valid for alginates with 39% and 63% guluronic content, for beads ranging from 11−30 mg and for beads air-dried at 20−75% relative humidity. The parameter t_c is easily estimated from the physical parameters of water vapor, the initial water content, and the relative humidity, in addition to an empirically derived correction factor, K. An explanation of this surprising fact might be that the surface of the bead is covered by a thin layer of free water. As this water evaporates, it is continuously renewed by fresh water expelled from the interior of the shrinking beads. The calcium alginate beads dry essentially as a water droplet.

Acknowledgment

The authors would like to thank Mr. Frank Fusiak from International Specialty Products (ISP) for providing the sodium alginate samples for experimental use.

Literature Cited

(1) King, A. H. Brown seaweed extracts (alginates). In: *Food hydrocolloids Vol II*; Glicksman, M., Ed.; CRC Press: Boca Raton, FL, 1983; pp 115−188.

(2) Sime, W. J. The practical utilization of alginates in food gelling systems. In: *Gums and Stabilisers for the Food Industry 2: Applications of Hydrocolloids;* Phillips, G. O.; Wedlock, D. J.; Williams, P. A., Eds.; Pergamon Press, Oxford, 1984; pp 177−188.

(3) Leach, G.; Oliveira, G.; Morais, R. Production of a carotenoid-rich product by alginate entrapment and fluid-bed drying of Dunaliella salina. *J Sci. Food Agri.* **1998**, *76*, 298–302.

(4) Wan, L. S. C.; Heng, P. W. S.; Chan, L. W. Drug encapsulation in alginate microspheres by emulsification. *J. Microencap.* **1992**, *9*, 309–316.

(5) Chan, L. W.; Jin, Y.; Heng, P. W. S. Cross-linking mechanisms of calcium and zinc in production of alginate microspheres. *Int. J. Pharm.* **2002**, *242*, 255–258.

(6) Annan, N. T.; Borza, A. D.; Hansen, L. T. Encapsulation in alginate-coated gelatin microspheres improves survival of the probiotic *Bifidobacterium adolescentis* 15703T during exposure to simulated gastro-intestinal conditions. *Food Res. Int.* **2008**, *41*, 184–193.

(7) Lim, F.; Sun, A. M. Microencapsulated islets as bioartificial endocrine pancreas. *Science* **1980**, *210*, 908–910.

(8) Russo, A.; Basaglia, M.; Tola, E.; Casella, S. Survival, root colonization and biocontrol capacities of Pseudomonas fluorescens F13 LacZY in dry alginate microbeads. *J. Indus. Microbiol. Biotechnol.* **2001**, *27*, 337–342.

(9) Grant, G. T.; Morris, E. S.; Rees, D. A.; Smith, P. J. C.; Thom, D. Biological interactions between polysaccharides and divalent cations: the egg-box model. *Febs. Letts.* **1973**, *32*, 195–198.

(10) Morris, E. R.; Rees, D. A.; Thom, D.; Boyd, J. Chiroptical and Stoichiometric Evidence of a Specific Primary Dimerisation Process in Alginate Gelation. *Carbohydr. Res.* **1978**, *66*, 145–154.

(11) Rees, D. A. Structure, conformation, and mechanism in the formation of polysaccharide gels and networks. *Ad. Carbohydr. Chem. Biochem.* **1969**, *24*, 267–332.

(12) Walker, H. L.; Connick, W. J., Jr. Sodium alginate for production and formulation of mycoherbicides. *Weed Sci.* **1983**, *31*, 333–338.

(13) Pillay, V.; Dangor, C. M.; Govender, T.; Moopanar, K. R.; Hurbans, N. Lonotropic gelation: Encapsulation of indomethacin in calcium alginate gel discs. *J. Microencap.* **1998**, *15*, 215–226.

(14) Champagne, C. P.; Gardner, N. J. The effect of protective ingredients on the survival of immobilized cells of Streptococcus thermophilus to air and freeze-drying. *Elec. J. Biotechnol* **2001**, *4* (3), 58–64.

(15) Li, X. Y.; Chen, X. G.; Liu, C. S.; Peng, H. N.; Cha, D. S. Effect of trehalose and drying process on the survival of encapsulated *Lactobacillus casei* ATCC 393. *Drying Technol.* **2008**, *26*, 895–901.

(16) Lee, K. Y.; Heo, T. R. Survival of *Bifidobacterium longum* immobilized in calcium alginate beads in simulated gastric juices and bile salt solution. *Appl. Environ. Microbiol.* **2000**, *66*, 869–873.

(17) Gbassi, G. K.; Vandamme, T.; Ennahar, S.; Marchioni, E. Microencapsulation of Lactobacillus plantarum spp in an alginate matrix coated with whey proteins. *Int. J. Food Microbiol.* **2009**, *129*, 103–105.

(18) Ross, G. R.; Gusils, C.; Gonzalez, S. N. Microencapsulation of probiotic strains for swine feeding. *Biol. Pharm. Bull.* **2008**, *31*, 2121–2125.

(19) Lemus, R. A.; Perez, M.; Andres, A.; Roco, T.; Tello, C. M.; Vega, A. Kinetic study of dehydration and desorption isotherms of red alga *Gracilaria*. *Food Sci. Technol.* **2008**, *41*, 1592–1599.

(20) Ding, W. K.; Shah, N. P. Effect of various encapsulation materials on the stability of probiotic bacteria. *J. Food Sci.* **2009**, *74*, 100–107.

(21) Zhang, J.; Datta, A. K. Some Considerations in Modeling of Moisture Transport in Heating of Hygroscopic Materials. *Drying Technol.* **2004**, *22*, 1983–2008.

(22) Chen, X. D. The Basics of a Reaction Engineering Approach to Modeling Air-Drying of Small Droplets or Thin-Layer Materials. *Drying Technol.* **2008**, *26*, 627–639.

(23) Saravacos, G. D.; Raouzeos, G. S. Diffusivity of moisture in air drying of starch gels. In: *Engineering and Food Vol. 1*, McKenna, B. M., Ed.; 1984, pp 499−507.

(24) Chen, X. D. A Discussion on a Generalized Correlation for Drying Rate Modeling. *Drying Technol.* **2005**, *23*, 415–426.

(25) Crank, J. *The Mathematics of Diffusion*; Clarendon Press: Oxford. 1956, pp. 347.

(26) Jost, W. *Diffusion in Solids, Liquids, Gases*; Academic Press: New York, 1952, p 558.

(27) Lee, H. C.; Oh, B. D.; Bae, S. W.; Kim, M. H.; Lee, J. Y.; Song, I. S. Partial Nucleate Boiling on the Microscale Heater Maintaining Constant Wall Temperature. *J. Nucl. Sci. Technol.* **2003**, *40*, 768.

(28) Perry, J. H., Ed. *Chemical Engineer's Handbook*, 4th ed.; McGraw-Hill, Inc.: New York, 1950, p 539.

(29) Lange, N. A. *Lange's Handbook of Chemistry*, Dean J. A., Ed.; McGraw-Hill, Inc: New York. 1999; pp 5−156.

(30) Gu, Z.; Alexandridis, P. Drying of films formed by ordered poly(ethylene oxide)−poly(propylene oxide) block copolymer gels. *Langmuir* **2005**, *21*, 1806–1817.

(31) Oyaas, J.; Storro, I.; Lysberg, M.; Svendsen, H.; Levine, D. W. Determination of effective diffusion coefficients and distribution constants in polysaccharide gels with non-steady-state measurements. *Biotechnol. Bioen.* **1995**, *47*, 501–507.

(32) Kim, S. W.; Bae, Y. H.; Okano, T. Hydrogels: swelling, drug loading, and release. *Pharm. Res.* **1992**, *9*, 283–290.

Received for review September 15, 2009
Revised manuscript received December 30, 2009
Accepted January 11, 2010

IE901451M